

Solving Fredholm Integro-Differential Equations Using Composite Numerical Integration and 7-Point Finite Differences Method

Surme Rasul Saber ¹, Younis Abid Sabawi ^{1*}, and Hoshman Qadir Hamad ¹

¹ Department of Mathematics, Faculty of Science and Health, Koya University, Koya KOY45, Kurdistan Region - F.R. Iraq

Article History

Received: 11.09.2025

Revised: 06.12.2025

Accepted: 17.12.2025

Published: 21.12.2025

Communicated by: Prof. Dr. Syed Abbas

*Email address:

younis.abid@koyauniversity.org

*Corresponding Author



Copyright: © 2024 by the author. Licensee Tishk International University, Erbil, Iraq. This article is an open-access article distributed under the terms and conditions of the Creative Commons Attribution License 4.0 (CC BY-4.0).

<https://creativecommons.org/licenses/by/4.0/>



Abstract: This paper presents a numerical solution to the Fredholm integro-differential equation (FIDEs) using the 7-point finite difference method combined with a quadrature rule and composite Boole's rule. The 7-point finite difference method effectively approximates the differential component, while the quadrature rule and Boole's rule address the integral component with enhanced accuracy. This approach optimizes computational efficiency and accuracy, demonstrating that the proposed method performs well for solving Fredholm integro-differential equations. The accuracy of the proposed scheme is rigorously evaluated using l^2 and l^∞ norms, while the computational efficiency is measured by assessing the CPU-time values, demonstrating a notable reduction in computational cost compared to traditional methods.

Keywords: Fredholm Integro-Differential Equation; Finite Difference Method; Quadrature Rule; Composite Boole's Rule.

1. Introduction

Fredholm integro-differential equations (FIDEs) arise in diverse scientific fields, including physics, biology, engineering, and economics, where phenomena involve both differential operators and memory effects described by integral terms. These equations typically take the form:

$$(1) \quad u''(x) + p u(x) = f(x) + \lambda \int_a^b k(x, t)u(t) dt,$$

with Dirichlet boundary conditions:

$$(2) \quad u(a) = \alpha, \quad u(b) = \beta$$

Solving FIDEs analytically is often infeasible for complex kernels $k(x, t)$ or inhomogeneous terms $f(x)$, necessitating robust numerical methods. While finite differences and quadrature rules are established tools for differential and integral operators separately, their synergistic integration remains critical for balancing accuracy, stability, and computational efficiency.

Existing approaches frequently employ low-order schemes (e.g., 2nd-order finite differences with Trapezoidal quadrature), limiting convergence rates and requiring fine discretization for acceptable accuracy. Recent advances focus on high-order approximations to improve efficiency. For instance,

6th-order finite difference schemes (e.g., 7-point stencils) offer superior derivative approximations, while composite Newton-Cotes quadrature's (e.g., Boole's rule) provide high-precision integral evaluations. However, a unified framework combining these high-order techniques for FIDEs—particularly addressing boundary effects and implementation efficiency has been underexplored.

Recent advances in numerical methods for FIDEs have focused on achieving higher orders of accuracy and computational efficiency. Homotopy perturbation and Variational iteration methods [1] Spectral methods, Legendre polynomial [2, 3] and Cubic B-spline finite element method [4] Haar wavelet-based approaches [5, 6] have been proposed for their excellent convergence properties. High-order compact finite difference schemes have been applied to FIDEs to improve accuracy, and for the Volterra integro-differential equation have used a compact finite difference method with the Haar wavelet method [7] has been used. Additionally, machine learning techniques with conventional methods like the trapezoidal rule [8] and Implicit-Explicit Rung-Kutta methods [9] have emerged as competitive alternatives. Furthermore, parallel computing implementations [10] have addressed a 9-point sixth-order accurate compact finite difference method. However, the combination of a 7-point finite difference scheme with composite quadrature rules (including Boole's rule) for Fredholm integro-differential equations, with a focus on boundary treatment and computational efficiency, has not been fully explored. This paper aims to fill this gap.

In this work, we introduce a novel numerical scheme that integrates 7-point finite differences for the differential component with composite quadrature rules (Boole's, Simpson's 3/8, and Trapezoidal) for the integral term.

The paper is structured as follows: Section 2 derives the unified discretization framework, Section 3 validates the method through numerical examples, and Section 4 discusses computational performance. Concluding remarks highlight applications and extensions.

2. Derivation of the Method [11, 12, 13]

To construct a numerical solution, we consider a partition $\Delta_N: a = x_0 < x_1 < \dots < x_{n-1} < x_n = b$ on a given interval $[a, b]$, where $h = x_{i+1} - x_i$ represents the mesh size of the partition, and let $H = \frac{b-a}{n}$ is the overall mesh size. We use a 7-point Finite difference on the differential parts combined with a quadrature rule and composite Boole's rule on the integral part of (1). Now using the quadrature rule and the composite Boole's rule with N subintervals and $x \in [a, b]$, The integral part of (1) is approximated by the Composite Simpson's 3/8, Trapezoidal rule, and Composite Boole's rule, respectively.

$$(3) \quad \int_a^b K_{i,j} u_j \, dx = \frac{3h}{8} \left((K_{i,0} u_0 + K_{i,N} u_N) + 3 \sum_{j=1}^{N-1} K_{i,j} u_j + 2 \sum_{j=1}^{\frac{N}{3}-1} K_{i,3j} u_{3j} \right)$$

$$(4) \quad \int_a^b K_{i,j} u_j \, dx = \frac{h}{2} \left((K_{i,0} u_0 + K_{i,N} u_N) + 2 \sum_{j=1}^{N-1} K_{i,j} u_j \right)$$

$$(5) \quad \int_a^b K_{i,j} u_j \, dx = \frac{2h}{45} \left(7(K_{i,0} u_0 + K_{i,N} u_N) + 32 \sum_{j=1}^{\frac{N}{2}} K_{i,2j-1} u_{2j-1} + 12 \sum_{j=1}^{\frac{N}{4}} K_{i,4j-2} u_{4j-2} + 14 \sum_{j=1}^{\frac{N}{4}-1} K_{i,4j} u_{4j} \right)$$

Where $k(x_i, t_j) = k_{i,j}$ and $u(x_i) = u_i$. using forward, central, and backward differences we can approximate the derivative part of (1) as

Forward finite difference, $i = 1, 2$,

$$(6) \quad u''(x) = \frac{812u_i - 3132u_{i+1} + 5265u_{i+2} - 5080u_{i+3} + 2970u_{i+4} - 972u_{i+5} + 137u_{i+6}}{180h^2}$$

Central finite difference $i = 3: n - 3$

$$(7) \quad u''(x) = \frac{2u_{i-3} - 27u_{i-2} + 270u_{i-1} - 490u_i + 270u_{i+1} - 27u_{i+2} + 2u_{i+3}}{180h^2} + O(h^6)$$

Backward finite difference $i = n - 2, n - 1$

$$(8) \quad u''(x) = \frac{812u_i - 3132u_{i-1} + 5265u_{i-2} - 5080u_{i-3} + 2970u_{i-4} - 972u_{i-5} + 137u_{i-6}}{180h^2}$$

2.1 7-Point Finite Difference Method with Composite Simpsons 3/8 Rule (FDCS)

by replacing $u''(x)$ in (1) with Composite Simpsons 3/8 rule (3) and (6-8), we have for $i = 1, 2$

$$(812 + 180q_i h^2)u_i - 3132u_{i+1} + 5265u_{i+2} - 5080u_{i+3} + 2970u_{i+4} - 972u_{i+5} + 137u_{i+6} \\ = 180h^2 f_i + \frac{135h^3}{2} (k_{i,0}u_0 + k_{i,N}u_N) + \frac{405h^3}{2} \sum_{j=1}^{N-1} k_{i,j}u_j + \frac{270h^3}{2} \sum_{j=1}^{\frac{N}{3}-1} k_{i,3j}u_{3j},$$

$i = 3: n - 3$

$$2u_{i-3} - 27u_{i-2} + 270u_{i-1} + (-490 + 180q_i h^2)u_i + 270u_{i+1} - 27u_{i+2} + 2u_{i+3} \\ = 180h^2 f_i + \frac{135h^3}{2} (k_{i,0}u_0 + k_{i,N}u_N) + \frac{405h^3}{2} \sum_{j=1}^{N-1} k_{i,j}u_j + \frac{270h^3}{2} \sum_{j=1}^{\frac{N}{3}-1} k_{i,3j}u_{3j} \\ \Rightarrow i = n - 2, n - 1$$

$$(812 + 180q_i h^2)u_i - 3132u_{i-1} + 5265u_{i-2} - 5080u_{i-3} + 2970u_{i-4} - 972u_{i-5} + 137u_{i-6} \\ = 180h^2 f_i + \frac{135h^3}{2} (k_{i,0}u_0 + k_{i,N}u_N) + \frac{405h^3}{2} \sum_{j=1}^{N-1} k_{i,j}u_j + \frac{270h^3}{2} \sum_{j=1}^{\frac{N}{3}-1} k_{i,3j}u_{3j}.$$

2.2 7-point Finite Difference Method with Composite Trapezoidal Rule (FDCT)

by replacing $u''(x)$ in (1) with Composite Trapezoidal rule (4) and (6-8), we have for $i = 1, 2$

$$(812 + 180q_i h^2)u_i - 3132u_{i+1} + 5265u_{i+2} - 5080u_{i+3} + 2970u_{i+4} - 972u_{i+5} + 137u_{i+6} \\ = 180h^2 f_i + 90h^3 (k_{i,0}u_0 + k_{i,N}u_N) + 180h^3 \sum_{j=1}^{N-1} k_{i,j}u_j,$$

$i = 3: n - 3$

$$2u_{i-3} - 27u_{i-2} + 270u_{i-1} + (-490 + 180q_i h^2)u_i + 270u_{i+1} - 27u_{i+2} + 2u_{i+3} \\ = 180h^2 f_i + 90h^3 (K_{i,0}U_0 + K_{i,N}U_N) + 180h^3 \sum_{j=1}^{N-1} k_{i,j}u_j,$$

$\Rightarrow i = n - 2, n - 1$

$$(812 + 180q_i h^2)u_i - 3132u_{i-1} + 5265u_{i-2} - 5080u_{i-3} + 2970u_{i-4} - 972u_{i-5} + 137u_{i-6} = 180h^2 f_i + 90h^3 (k_{i,0}u_0 + k_{i,N}u_N) + 180h^3 \sum_{j=1}^{N-1} k_{i,j}u_j.$$

2.3 7-point Finite Difference Method with Composite Boole's Rule (FDCH)

and by replacing $u''(x)$ in (1) with Composite Boole's rule (4) and (6-8), we have for $i = 1, 2$

$$(812 + 180q_i h^2)u_i + -3132u_{i+1} + 5265u_{i+2} - 5080u_{i+3} + 2970u_{i+4} - 972u_{i+5}$$

$$+137u_{i+6} = 180h^2 f_i + 56h^3 (k_{i,0}u_0 + k_{i,N}u_N) + 256h^3 \sum_{j=1}^{N/2} k_{i,2j-1}u_{2j-1} + \\ 96h^3 \sum_{j=1}^{\frac{N}{4}} k_{i,4j-2}u_{4j-2} + 112h^3 \sum_{j=1}^{\frac{N}{4}-1} k_{i,4j}u_{4j},$$

$i = 3: n - 3$

$$2u_{i-3} - 27u_{i-2} + 270u_{i-1} + (-490 + 180q_i h^2)u_i + 270u_{i+1} - 27u_{i+2} + 2u_{i+3}$$

$$= 180h^2 f_i + 56h^3 (k_{i,0}u_0 + k_{i,N}u_N) + 256h^3 \sum_{j=1}^{N/2} k_{i,2j-1}u_{2j-1} + 96h^3 \sum_{j=1}^{\frac{N}{4}} k_{i,4j-2}u_{4j-2} + \\ 112h^3 \sum_{j=1}^{\frac{N}{4}-1} k_{i,4j}u_{4j},$$

$\Rightarrow i = n - 2, n - 1$

$$(812 + 180q_i h^2)u_i - 3132u_{i-1} + 5265u_{i-2} - 5080u_{i-3} + 2970u_{i-4} - 972u_{i-5}$$

$$+137u_{i-6} = 180h^2 f_i + 56h^3 (K_{i,0}U_0 + K_{i,N}U_N) + 256h^3 \sum_{j=1}^{N/2} K_{i,2j-1}U_{2j-1} + \\ 96h^3 \sum_{j=1}^{\frac{N}{4}} K_{i,4j-2}U_{4j-2} + 112h^3 \sum_{j=1}^{\frac{N}{4}-1} K_{i,4j}U_{4j}.$$

3. Convergence Analysis

This section aims to prove the convergence analysis of the 7-Point Finite Difference Method. We first introduce the following lemma that plays a crucial role in the proof. We define the space $L_2(a, b)$ represents a Hilbert space with the inner product:

$$(u(x), v(x)) = \int_a^b u(x) \cdot v(x) \, dx.$$

The Sobolev H^1 and H^2 admit a natural norm

$$\|u\|_{S^1}^2 = \|u\|^2 + \|u'\|^2, \|v\|_{S^2}^2 = \|v\|^2 + \|v'\|^2$$

Lemma 3.1: The remainder \mathcal{T}^{SM} of the composite Boole's rule satisfies

$$|\mathcal{T}^{SM}| \leq \frac{-8}{945} h^4 u^6(\xi).$$

Proof: Let the function $w_1 = K(x_i, z)u(z)$ be continuous and possesses a continuous derivative in $[z_0, z_2]$. Expanding y about $z = z_0$ we obtain

$$w_1(x) = w_{10} + (z - z_0)w_{10}' + \frac{1}{2}(z - z_0)^2 w_{10}'' + \frac{1}{3!}(z - z_0)^3 w_{10}''' + \frac{1}{4!}(z - z_0)^3 w_{10}^{(iv)} + \dots$$

$$\int_{s_0}^{s_2} K(x_i, z)u(z) \, dz = \int_0^2 h \left(w_{10} + rh w_{10}' + \frac{(rh)^2}{2} w_{10}'' + \frac{(rh)^3}{3!} w_{10}''' + \frac{(rh)^4}{4!} w_{10}^{(iv)} + \dots \right) dr$$

$$\begin{aligned}
&= h[rw_{10} + \frac{r^2 h}{2} w_{10}' + \frac{(rh)^2}{6} p w_{10}'' + \frac{(rh)^3}{24} p w_{10}''' + \frac{(rh)^4}{120} r w_{10}^{(iv)} + \dots]^2 \\
(9) \quad &= 2hw_{10} + 2h^2 w_{10}' + \frac{4h^2}{3} w_{10}'' + \frac{2h^4}{3} w_{10}''' + \frac{4h^5}{15} w_{10}^{(iv)} + \dots
\end{aligned}$$

Therefore,

$$(10) \quad w_{10} = w_{10}$$

$$(11) \quad w_{11} = w_{10} + hw_{10}' + \frac{h^2}{2} w_{10}'' + \frac{h^3}{6} w_{10}''' + \frac{h^4}{24} w_{10}^{(iv)} + \dots$$

$$(12) \quad w_{12} = w_{10} + 2hw_{10}' + 2h^2 w_{10}'' + \frac{4h^3}{3} w_{10}''' + \frac{2h^4}{3} w_{10}^{(iv)} + \dots$$

Combining 9-12 becomes

$$\begin{aligned}
\frac{h}{3} [w_{10} + 4w_{11} + w_{12}] &= \frac{h}{3} \left[6w_{10} + 6hw_{10}' + 4h^2 w_{10}'' + 2h^3 w_{10}''' + \frac{5h^4}{6} w_{10}^{(iv)} + \dots \right] \\
(13) \quad &= 2hw_{10} + 2h^2 w_{10}' + \frac{4h^3}{3} w_{10}'' + \frac{2h^4}{3} w_{10}''' + \frac{5h^4}{18} w_{10}^{(iv)} + \dots
\end{aligned}$$

Using 9 and (13), these leads

$$\int_{s_0}^{s_2} w_1 ds - \frac{h}{3} [w_{10} + 4w_{11} + w_{12}] = \frac{4}{472.5} h^5 w_{10}^6,$$

The composite Boole's rule is a numerical integration method used to approximate the definite integral of a function over an interval by dividing the interval into multiple sub-intervals and applying Boole's rule on each sub-interval. To use this method, the interval of integration $[0, l]$ is subdivided into N even subdivisions as follows: $0 = z_0 < z_1 < z_2 < \dots < z_N = l$. The integral over the entire interval $[0, l]$ can be approximated by summing up the individual integrals over each sub-interval using the composite Boole's rule. The formula for the composite Boole's rule for a sub-interval $[z_i, z_{i+1}]$ is given by:

$$\begin{aligned}
\int_{s_0}^{s_n} w_1 ds &= \frac{2h}{45} \left[7w_{10} + 32 \sum_{j=1}^{\frac{N}{2}} w_{12j-1} + 12 \sum_{j=1}^{\frac{N}{4}} w_{14j-2} + 14 \sum_{j=1}^{\left(\frac{N}{4}\right)-1} w_{14j} + 7w_{1N} \right] = \\
&\frac{4}{472.5} h^5 w_{10}^{(6)},
\end{aligned}$$

We obtain the errors in the intervals $[0, l]$ as

$$T^{SM} = \frac{4}{472.5} h^5 [w_0^{(6)} + w_2^{(6)} + \dots + w_{N-2}^{(6)}] = \frac{8}{945} h^4 w^{(6)}(\xi), \quad \xi \in [0, l].$$

Assumption 1: The kernel functions $k(x, z)$ satisfies the following positive definite property:

$$(14) \quad \int_a^b \int_a^b (k(x, z) \Phi(x), \Phi(z)) dx dz > 0.$$

for every continuous $\Phi(x) = (\Phi_1(x), \Phi_2(x), \dots, \Phi_k(x)) \neq 0$, and the integral

$$\int_a^b \int_a^b |k(x, z)|^2 dx dz < \infty.$$

Theorem 3.2 (Error estimates): Assuming that assumption 1 is satisfied and the kernel functions $k(x, z)$ is smooth enough, then

$$(15) \quad \|u(x) - \theta_h(x)\|_{s^1} \leq Ch^4$$

where $C > 0$.

Proof: Setting $e_h = u - \theta_h(x)$ in (1), gives

$$(16) \quad e_h'' + pe_h - \gamma_1 \int_a^b (k(x, z) e_h) ds = f(x) + \mathcal{T}(x, h)$$

where $\mathcal{T}(x, h)$ be a vector denoting the truncation error such that

$$\mathcal{T}(x, h) = -\theta_h'' - p\theta_h + \lambda \int_a^b (k(x, z) \theta_h(z)) dz$$

Then, we have

$$\mathcal{T}(x_i, h) = -L_h w_i + \lambda \int_a^b (k(x_i, z) w(z)) dz - \theta_h'' - p\theta_h + L_h w_i - \lambda \int_a^b (k(x, z) (w(z) - \theta_h(z))) dz = O(h^4).$$

Multiplying Eq. (16) by e_{1h} and integrating with respect to x , gives

$$\int_a^b (e_h'', e_h) dx + \int_a^b p(e_h, e_h) dx - \lambda \int_a^b \int_a^b (k(x, z) (e_h, e_h)) dz dx = \int_a^b (f(x), e_h) dx + \int_a^b (\mathcal{T}(x, h), e_h) dx.$$

Since $p - \frac{1}{2}q'' \geq 0$ and integrating by parts along with Assumption 1, we have

$$\int_a^b (e_h', e_h') dx \leq \int_a^b (f(x), e_h) dx + \int_a^b (\mathcal{T}(x, h), e_h) dx.$$

Applying Cauchy's inequality and Lemma 3.1, this becomes

$$\|e_h\|_{s^1}^2 \leq \|f(x)\| \|e_h\|_{s^1} \|\mathcal{T}(x, h)\| \|e_h\|_{s^1},$$

By taking small values of $h^4 > h^6$, the proof will be finished.

4. Results and Discussion

The section illustrates the performance of the presented method through an implementation based on MATLAB programming. The error norms of l^2 and l^∞ are used to measure the error between the numerical and analytical solutions. We will verify that the presented method can be applied with a large number of N . The presented methods are convergence because when N is increasing in the error in solutions is also decreasing. We denote by E errors terms given by:

$$E(x) = u(x) - U_{Appr.}(x)$$

Let us introduce the three accuracy indicators when using the space step size h , as follows:

- The Absolute (pointwise) error is:

$$E(x) = |E(x_i)|$$

- The l^∞ -norm and l^2 -norm of the error as:

$$l^\infty(E, h) = \max_{0 \leq i \leq N} |E(x_i)|, \quad l^2(E, h) = \sqrt{h \sum_{i=0}^N |E(x_i)|^2}$$

- The order of convergence R is calculated as:

$$Rate = \frac{\log(\text{Error(N1)}/\text{Error(N2)})}{\log(N2/N1)}$$

Example 1: Consider the FIDE:

$$u''(x) + u(x) = x + 1 - 2e^x - 4e^{x-2} + \int_0^2 e^{x-t} u(t) dt,$$

with Dirichlet boundary conditions: $u(0) = 1$, $u(1) = 3$,

and the exact solution is $u(x) = x + 1$.

Table 1: Numerical results for Example 1 by using FDCB, FDGS, and FDCT with $N = 12$ and $0 \leq x \leq 2$.

| x_i | $u(x)$ | $U_{\text{Appro.}}(x)$ FDCB | $U_{\text{Appro.}}(x)$ FDGS | $U_{\text{Appro.}}(x)$ FDCT |
|------------------|------------|--------------------------------|--------------------------------|--------------------------------|
| 0.1667 | 1.1667e+00 | 1.1667e+00 | 1.1667e+00 | 1.1668e+00 |
| 0.3333 | 1.3333e+00 | 1.3333e+00 | 1.3333e+00 | 1.3337e+00 |
| 0.5000 | 1.5000e+00 | 1.5000e+00 | 1.5000e+00 | 1.5005e+00 |
| 0.6667 | 1.6667e+00 | 1.6667e+00 | 1.6667e+00 | 1.6672e+00 |
| 0.8333 | 1.8333e+00 | 1.8333e+00 | 1.8333e+00 | 1.8340e+00 |
| 1.0000 | 2.0000e+00 | 2.0000e+00 | 2.0000e+00 | 2.0007e+00 |
| 1.1667 | 2.1667e+00 | 2.1667e+00 | 2.1667e+00 | 2.1674e+00 |
| 1.3333 | 2.3333e+00 | 2.3333e+00 | 2.3333e+00 | 2.3340e+00 |
| 1.5000 | 2.5000e+00 | 2.5000e+00 | 2.5000e+00 | 2.5006e+00 |
| 1.6667 | 2.6667e+00 | 2.6667e+00 | 2.6667e+00 | 2.6671e+00 |
| 1.8333 | 2.8333e+00 | 2.8333e+00 | 2.8333e+00 | 2.8336e+00 |
| $l^2(E, h)$ | | 1.8739e-07 | 2.1560e-05 | 7.0978e-04 |
| $l^\infty(E, h)$ | | 1.8288e-07 | 2.1041e-05 | 6.9271e-04 |
| CPU-time | | 1.026330 | 1.403556 | 1.808207 |

Table 2: Rate Convergence of FDCB, FDCS, and FDCT for $l^2(E, h)$ in Example 1.

| N | FDCB–$l^2(E, h)$ | Rate | FDCS–$l^2(E, h)$ | Rate | FDCT–$l^2(E, h)$ | Rate |
|-----------------------|------------------------------------|-------------|------------------------------------|-------------|------------------------------------|-------------|
| 12 | 1.8739e-07 | | 2.1560e-05 | | 7.0978e-04 | |
| 24 | 7.3999e-09 | 4.6624 | 1.3600e-06 | 3.9867 | 1.7729e-04 | 2.0013 |
| 48 | 4.6834e-11 | 7.3038 | 8.5195e-08 | 3.9967 | 4.4312e-05 | 2.0003 |
| 96 | 5.3381e-13 | 6.4551 | 5.3273e-09 | 3.9993 | 1.1077e-05 | 2.0001 |

Table 3: Rate Convergence of FDCB, FDCS, and FDCT for $l^\infty(E, h)$ in Example 1.

| N | FDCB–$l^\infty(E, h)$ | Rate | FDCS–$l^\infty(E, h)$ | Rate | FDCT–$l^\infty(E, h)$ | Rate |
|-----------------------|---|-------------|---|-------------|---|-------------|
| 12 | 1.8288e-07 | | 2.1041e-05 | | 6.9271e-04 | |
| 24 | 2.9165e-09 | 5.9705 | 1.3334e-06 | 3.9800 | 1.7383e-04 | 1.9946 |
| 48 | 4.5856e-11 | 5.9910 | 8.3531e-08 | 3.9967 | 4.3447e-05 | 2.0003 |
| 96 | 8.6686e-13 | 5.7252 | 5.2248e-09 | 3.9989 | 1.0864e-05 | 1.9997 |

Example 2: Consider the FIDE:

$$u''(x) + 6u(x) = 5 \sin x + 6\pi^2 \cos x + \frac{3}{2} \int_0^{2\pi} \cos x t^2 u(t) dt,$$

with Dirichlet boundary conditions: $u(0) = 1$, $u(2\pi) = 0$,

and the exact solution is $u(x) = \sin x$.

Table 4: Rate Convergence of FDCB, FDCS, and FDCT for $l^2(E, h)$ in Example 2.

| N | FDCB–$l^2(E, h)$ | Rate | FDCS–$l^2(E, h)$ | Rate | FDCT–$l^2(E, h)$ | Rate |
|-----------------------|------------------------------------|-------------|------------------------------------|-------------|------------------------------------|-------------|
| 12 | 6.4346e-02 | | 7.2330e-02 | | 2.7093e+01 | |
| 24 | 6.4087e-04 | 6.6497 | 6.4183e-04 | 6.8163 | 3.6328e-02 | 9.5426 |
| 48 | 1.2291e-05 | 5.7044 | 1.9853e-05 | 5.0148 | 6.7694e-03 | 2.4240 |
| 96 | 1.1399e-07 | 6.7526 | 1.0740e-06 | 4.2083 | 1.6792e-03 | 2.0113 |

Table 5: Numerical results for Example 2 by using FDCB, FDCS, and FDCT with $N = 12$ and $0 \leq x \leq 2\pi$.

| x_i | $\mathbf{u}(x)$ | $\mathbf{U}_{Appr.}(x)$ | $\mathbf{U}_{Appr.}(x)$ | $\mathbf{U}_{Appr.}(x)$ |
|------------------|-----------------|-------------------------|-------------------------|-------------------------|
| | | FDCB | FDCS | FDCT |
| 0.5236 | 5.0000e-01 | 5.4364e-01 | 5.4844e-01 | 5.0000e-01 |
| 1.0472 | 8.6603e-01 | 8.7175e-01 | 8.7449e-01 | 8.6603e-01 |
| 1.5708 | 1.0000e+00 | 9.8947e-01 | 9.8938e-01 | 1.0000e+00 |
| 2.0944 | 8.6603e-01 | 8.5574e-01 | 8.5302e-01 | 8.6603e-01 |
| 2.6180 | 5.0000e-01 | 4.8396e-01 | 4.7944e-01 | 5.0000e-01 |
| 3.1416 | 1.2246e-16 | -3.4861e-02 | -4.0008e-02 | 1.2246e-16 |
| 3.6652 | -5.0000e-01 | -5.4524e-01 | -5.4977e-01 | -5.0000e-01 |
| 4.1888 | -8.6603e-01 | -8.9267e-01 | -8.9540e-01 | -8.6603e-01 |
| 4.7124 | -1.0000e+00 | -9.9056e-01 | -9.9064e-01 | -1.0000e+00 |
| 5.2360 | -8.6603e-01 | -8.3473e-01 | -8.3199e-01 | -8.6603e-01 |
| 5.7596 | -5.0000e-01 | -4.7865e-01 | -4.7386e-01 | -5.0000e-01 |
| $l^2(E, h)$ | | 6.4346e-02 | 7.2330e-02 | 2.7093e+01 |
| $l^\infty(E, h)$ | | 4.5245e-02 | 4.9769e-02 | 1.6100e+01 |
| CPU-time | | 1.390582 | 2.399016 | 1.731279 |

Table 6: Rate Convergence of FDCB, FDCS, and FDCT for $l^\infty(E, h)$ in Example 2.

| N | $\mathbf{FDCB}-l^\infty(E, h)$ | Rate | $\mathbf{FDCS}-l^\infty(E, h)$ | Rate | $\mathbf{FDCT}-l^\infty(E, h)$ | Rate |
|-----|--------------------------------|--------|--------------------------------|--------|--------------------------------|--------|
| 12 | 4.5245e-02 | | 4.9769e-02 | | 1.6100e+01 | |
| 24 | 4.3169e-04 | 6.7116 | 4.3341e-04 | 6.8434 | 3.3738e-02 | 8.8985 |
| 48 | 7.1335e-06 | 5.9192 | 1.2882e-05 | 5.0723 | 6.7694e-03 | 2.3173 |
| 96 | 6.6993e-08 | 6.7345 | 7.1893e-07 | 4.1634 | 1.6792e-03 | 2.0113 |

Example 3: Consider the FIDE:

$$u''(x) + 8u(x) = 9e^x - x^4 + \int_0^1 x^4 t u(t) dt,$$

with Dirichlet boundary conditions: $u(0) = 1$, $u(1) = e^1$,

and the exact solution is $\mathbf{u}(x) = e^x$.

Table 7: Numerical results for Example 3 by using FDDB, FDGS, and FDCT with $N = 12$ and $0 \leq x \leq 1$.

| x_i | $u(x)$ | $U_{Appr.}(x)$ | $U_{Appr.}(x)$ | $U_{Appr.}(x)$ |
|------------------|------------|----------------|----------------|----------------|
| | | FDDB | FDGS | FDCT |
| 0.0833 | 1.0000e+00 | 1.0869e+00 | 1.0869e+00 | 1.0000e+00 |
| 0.1667 | 1.0869e+00 | 1.1814e+00 | 1.1814e+00 | 1.0868e+00 |
| 0.2500 | 1.1814e+00 | 1.2840e+00 | 1.2840e+00 | 1.1813e+00 |
| 0.3333 | 1.2840e+00 | 1.3956e+00 | 1.3956e+00 | 1.2839e+00 |
| 0.4167 | 1.3956e+00 | 1.5169e+00 | 1.5169e+00 | 1.3954e+00 |
| 0.5000 | 1.5169e+00 | 1.6487e+00 | 1.6487e+00 | 1.5167e+00 |
| 0.5833 | 1.6487e+00 | 1.7920e+00 | 1.7920e+00 | 1.6485e+00 |
| 0.6667 | 1.7920e+00 | 1.9477e+00 | 1.9477e+00 | 1.7918e+00 |
| 0.7500 | 1.9477e+00 | 2.1170e+00 | 2.1170e+00 | 1.9475e+00 |
| 0.8333 | 2.1170e+00 | 2.3010e+00 | 2.3010e+00 | 2.1168e+00 |
| 0.9167 | 2.3010e+00 | 2.5009e+00 | 2.5009e+00 | 2.3008e+00 |
| $l^2(E, h)$ | | 4.7879e-07 | 3.6324e-07 | 1.6634e-04 |
| $l^\infty(E, h)$ | | 7.6221e-07 | 6.1779e-07 | 2.2994e-04 |
| CPU-time | | 1.718053 | 2.081650 | 1.849899 |

Table 8: Rate Convergence of FDDB, FDGS, and FDCT for $l^2(E, h)$ in Example 3.

| N | $FDDB-l^2(E, h)$ | Rate | $FDGS-l^2(E, h)$ | Rate | $FDCT-l^2(E, h)$ | Rate |
|-----|------------------|--------|------------------|--------|------------------|--------|
| 12 | 4.7879e-07 | | 3.6324e-07 | | 1.6634e-04 | |
| 24 | 7.3999e-09 | 6.0157 | 1.2683e-08 | 4.8400 | 4.1613e-05 | 1.9990 |
| 48 | 7.3900e-11 | 6.6458 | 1.1308e-09 | 3.4875 | 1.0405e-05 | 1.9998 |
| 96 | 2.0648e-12 | 5.1615 | 7.5390e-11 | 3.9068 | 2.6012e-06 | 2.0000 |

Table 9: Rate Convergence of FDCB, FDCS, and FDCT for $l^\infty(E, h)$ in Example 3.

| N | $\mathbf{FDCB}-l^\infty(E, h)$ | Rate | $\mathbf{FDCS}-l^\infty(E, h)$ | Rate | $\mathbf{FDCT}-l^\infty(E, h)$ | Rate |
|-----------------------|--|-------------|--|-------------|--|-------------|
| 12 | 7.6221e-07 | | 6.1779e-07 | | 2.2994e-04 | |
| 24 | 1.0221e-08 | 6.2206 | 1.7626e-08 | 5.1313 | 5.7960e-05 | 1.9881 |
| 48 | 1.0088e-10 | 6.6628 | 1.5760e-09 | 3.4834 | 1.4492e-05 | 1.9998 |
| 96 | 2.9916e-12 | 5.0756 | 1.0506e-10 | 3.9070 | 3.6230e-06 | 2 |

Example 4: Consider the FIDE:

$$u''(x) + 2u(x) = \cos x + 2x - \left(-2 + \frac{\pi^3}{3}\right) \sin x + \int_0^\pi \sin x \, t \, u(t) \, dt,$$

with Dirichlet boundary conditions: $u(0) = 1$, $u(\pi) = 1 + \pi$,

and the exact solution is $u(x) = \cos x + x$.

Table 10: Numerical results for Example 4 by using FDCB, FDCS, and FDCT with $N = 12$ and $0 \leq x \leq \pi$.

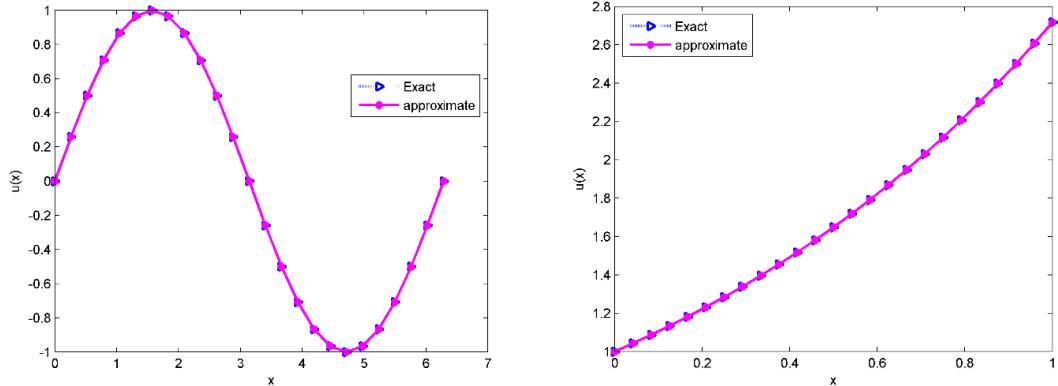
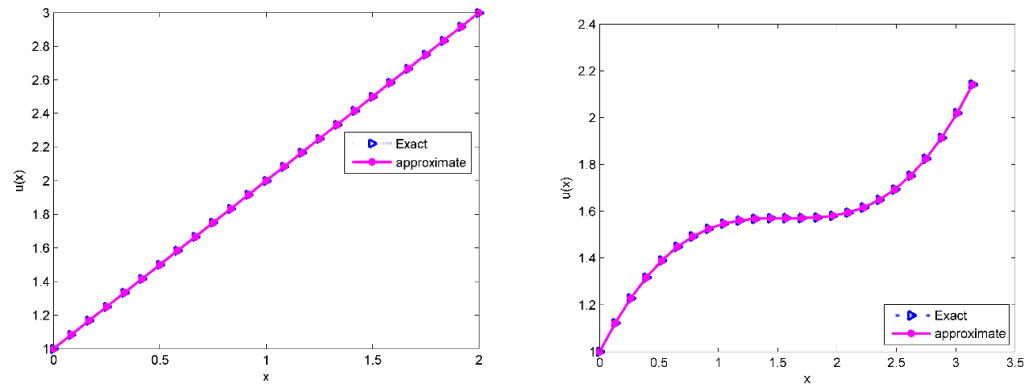
| x_i | $u(x)$ | $U_{Appro.}(x)$ | $U_{Appro.}(x)$ | $U_{Appro.}(x)$ |
|------------------------------------|--------------------------|-----------------------------------|-----------------------------------|-----------------------------------|
| | | FDCB | FDCS | FDCT |
| 0.2618 | 1.2277e+00 | 1.2261e+00 | 1.2261e+00 | 1.2232e+00 |
| 0.5236 | 1.3896e+00 | 1.3877e+00 | 1.3877e+00 | 1.3820e+00 |
| 0.7854 | 1.4925e+00 | 1.4905e+00 | 1.4904e+00 | 1.4824e+00 |
| 1.0472 | 1.5472e+00 | 1.5453e+00 | 1.5452e+00 | 1.5354e+00 |
| 1.3090 | 1.5678e+00 | 1.5662e+00 | 1.5661e+00 | 1.5552e+00 |
| 1.5708 | 1.5708e+00 | 1.5696e+00 | 1.5695e+00 | 1.5582e+00 |
| 1.8326 | 1.5738e+00 | 1.5731e+00 | 1.5730e+00 | 1.5621e+00 |
| 2.0944 | 1.5944e+00 | 1.5942e+00 | 1.5941e+00 | 1.5843e+00 |
| 2.3562 | 1.6491e+00 | 1.6494e+00 | 1.6493e+00 | 1.6413e+00 |
| 2.6180 | 1.7520e+00 | 1.7527e+00 | 1.7526e+00 | 1.7469e+00 |
| 2.8798 | 1.9139e+00 | 1.9149e+00 | 1.9148e+00 | 1.9119e+00 |
| $l^2(E, h)$ | | 2.2710e-03 | 2.3927e-03 | 1.5906e-02 |
| $l^\infty(E, h)$ | | 1.9887e-03 | 2.0902e-03 | 1.5906e-02 |
| CPU-time | | 0.991248 | 0.998566 | 1.079159 |

Table 11: Rate Convergence of FDCB, FDCS, and FDCT for $l^2(E, h)$ in Example 4.

| N | FDCB–$l^2(E, h)$ | Rate | FDCS–$l^2(E, h)$ | Rate | FDCT–$l^2(E, h)$ | Rate |
|-----------------------|------------------------------------|-------------|------------------------------------|-------------|------------------------------------|-------------|
| 12 | 2.2710e-03 | | 2.3927e-03 | | 1.5906e-02 | |
| 24 | 1.1469e-05 | 7.6294 | 2.2262e-05 | 6.7479 | 3.5927e-03 | 2.1464 |
| 48 | 4.7253e-08 | 7.9231 | 8.3936e-07 | 4.7291 | 8.9521e-04 | 2.0048 |
| 96 | 1.8037e-10 | 8.0333 | 5.0487e-08 | 4.0553 | 2.2372e-04 | 2.0005 |

Table 12: Rate Convergence of FDCB, FDCS, and FDCT for $l^\infty(E, h)$ in Example 4.

| N | FDCB–$l^\infty(E, h)$ | Rate | FDCS–$l^\infty(E, h)$ | Rate | FDCT–$l^\infty(E, h)$ | Rate |
|-----------------------|---|-------------|---|-------------|---|-------------|
| 12 | 1.9887e-03 | | 2.0902e-03 | | 1.5906e-02 | |
| 24 | 9.9386e-06 | 7.6446 | 1.8466e-05 | 6.8226 | 2.8665e-03 | 2.4722 |
| 48 | 4.0761e-08 | 7.9297 | 6.7008e-07 | 4.7844 | 7.1427e-04 | 2.0047 |
| 96 | 1.5487e-10 | 8.0400 | 4.0282e-08 | 4.0561 | 1.7851e-04 | 2.0005 |

Figure 1: Exact and Approximate Solution of Examples 1 and 2 using $N = 24, h = 0.0833$ and $h = 0.2618$.Figure 2: Exact and Approximate solutions of Examples 3 and 4 using $N = 24$ and $h = 0.417$ and $h = 0.1309$.

These figures would visually demonstrate the perfect agreement between the exact solutions $u(x) = x + 1$, $u(x) = \sin(x)$ and the numerical approximations obtained by the FDCB method for $N = 24$. The curves for the exact and approximate solutions would be virtually indistinguishable, graphically confirming the high accuracy quantified in Tables 1 and 5.

Similarly, this figure would show the plot of $u(x) = e^x$ and $u(x) = \cos x + x$ and its FDCB approximation. The close overlap of these curves would provide visual validation of the excellent results shown in Tables 7 and 10 for Examples 3 and 4.

5. Conclusion

This paper demonstrates that combining a high-order 7-point finite difference method with composite Boole's rule (the FDCB method) is a highly effective strategy for solving Fredholm integro-differential equations. The results show that this approach is not only more accurate but also often faster than using lower-order methods like those based on the Trapezoidal or Simpson's rules. This is because the high-order FDCB method achieves excellent precision with a coarser grid, reducing the overall size of the problem and leading to lower computational times. The FDCB scheme provides a superior balance of speed and accuracy. It is a robust and efficient numerical technique that outperforms traditional methods, making it a highly recommended choice for solving these types of equations. We plan to investigate the use of the B-spline collocation method for solving fractional-order Fredholm integro-differential equations, as this technique shows strong potential for achieving higher numerical accuracy. For more details, see [14].

Author's Contribution

"We confirm that all named authors have read and approved the manuscript. We also confirm that each author has the same contribution to the paper. We further confirm that all authors have approved the order of authors listed in the manuscript."

Conflict of Interest: *"There is no conflict of interest for this paper."*

Acknowledgment: *The authors would like to express their gratitude to Koya University for its financial support.*

References

- [1] N. A. Mohammad, Y. A. Sabawi and M. S. Hasso, "Error Estimation and Approximate Solution of Nonlinear Fredholm Integro-Differential Equations," Palestine Journal of Mathematics, vol. 13, no. 3, 2024.
- [2] Y. Talaei, S. Noeiaghdam and H. Hosseinzadeh, "Numerical solution of fractional order fredholm integro-differential equations by spectral method with fractional basis functions," Известия Иркутского государственного университета, vol. 45, pp. 89-103, 2023. <https://doi.org/10.26516/1997-7670.2023.45.89>
- [3] S. Yalçınbaş, M. Sezer and H. H. Sorkun, "Legendre polynomial solutions of high-order linear Fredholm integro-differential equations," Applied Mathematics and Computation, vol. 210, no. 2, pp. 334-349, 2009. <https://doi.org/10.1016/j.amc.2008.12.090>
- [4] Y. A. Sabawi and B. O. Hussen, "A cubic B-spline finite element method for Volterra integro-differential equation," Palestine Journal of Mathematics, vol. 13, no. 3, pp. 571-583, 2024.
- [5] N. A. Mohammad, Y. A. Sabawi and M. S. Hasso, "Haar wavelet method for the numerical solution of nonlinear Fredholm integro-differential equations," Journal of Education and Science, vol. 32, no. 4, pp. 10-25, 2023. <https://doi.org/10.33899/edusj.2023.139892.1360>

- [6] N. A. Mohammad, Y. A. Sabawi and M. S. Hasso, "Numerical solution based on the Haar wavelet collocation method for partial integro-differential equations of Volterra type," *Arab Journal of Basic and Applied Sciences*, vol. 31, no. 1, pp. 614-628, 2024. <https://doi.org/10.1080/25765299.2024.2419145>
- [7] N. A. Mohammad, Y. A. Sabawi and M. S. Hasso, "A compact finite-difference and Haar wavelets collocation technique for parabolic volterra integro-differential equations," *Physica Scripta*, vol. 99, no. 12, p. 125251, 2024. <https://doi.org/10.1088/1402-4896/ad8d3d>
- [8] A. Harbi, Z. N. Kazem and S. E. Mohammed, "Advancements in Numerical Analysis: Techniques for Solving Volterra and Fredholm Equations," *Journal of Al-Qadisiyah for Computer Science and Mathematics*, vol. 17, no. 2, pp. 80-91, 2025. <https://doi.org/10.29304/jqcsm.2025.17.22211>
- [9] M. A. Pirdawood, H. M. Rasool, Y. A. Sabawi and B. F. Aziz, "Mathematical modeling and analysis for COVID-19 model by using implicit-explicit Rung-Kutta methods," *Academic Journal of Nawroz University*, vol. 11, no. 3, pp. 65-73, 2022. <https://doi.org/10.25007/ajnu.v11n1a1244>
- [10] M. Nabavi, M. H. Kamran Siddiqui and J. Dargahi, "A new 9-point sixth-order accurate compact finite-difference method for the Helmholtz equation," *Journal of Sound and Vibration*, vol. 307, pp. 972-982, 2007. <https://doi.org/10.1016/j.jsv.2007.06.070>
- [11] H. Nyengeri, J. J. Sinzingayo, D. Bonaventure and N. Eugène , "Effect of Asymmetric Finite Difference Formulas on the Orders of Central Difference Approximations for the Second Derivative of a Periodic Function," *Open Access Library Journal*, vol. 10, no. 11, pp. 1-11, 2023. <https://doi.org/10.4236/oalib.1110875>
- [12] K. R. Ishtiaq and R. Ohba, "Closed-form expressions for the finite difference approximations of first and higher derivatives based on Taylor series," *Journal of Computational and Applied Mathematics*, vol. 107, no. 2, pp. 179-193, 1999. [https://doi.org/10.1016/S0377-0427\(99\)00088-6](https://doi.org/10.1016/S0377-0427(99)00088-6)
- [13] R. M. Siddiqur, M. P. Moushumi and M. A. Abul Kalam , "Comparison of the methods for numerical integration," *Jahangirnagar University Journal of Science*, vol. 42, no. 2, pp. 63-78, 2019.
- [14] Y. A. Sabawi and H. Q. Hamad, "Numerical solution of the Whitham-Broer-Kaup shallow water equation by quartic B-spline collocation method," *Physica Scripta*, vol. 99, no. 1, pp. 1-17, 2023. <https://doi.org/10.1088/1402-4896/ad1561>